

# Two-Dimensional Isotropic NMR of Quadrupole Nuclei in Solids

AGO SAMOSON

*Institute of Chemical Physics and Biophysics, Akadeemia Tee 23, Tallinn EE0026, Estonia*

Received April 23, 1996; revised May 28, 1996

A recent demonstration of multiquantum NMR of quadrupole nuclei in solids leads to new interesting possibilities in analytical spectroscopy. One-dimensional high-resolution spectra without any anisotropic second- or fourth-rank line broadening were recorded, using a sample spinning about a single constant angle with the magnetic field ( $I$ ). The suppression of the second anisotropic component was effectively achieved by implementation of a parametric evolution time. The same averaging effect can be achieved in real time with the double-rotation sample reorientation technique (2). In both cases, spectra remain field dependent, with the center of gravity of the line determined by the combination of quadrupole interaction and chemical shift. A field-independent interpretation of spectra is in principle possible with numerical analyses using either DOR sidebands or a 2D representation of multiquantum MAS spectra (3, 4), or repeated measurements at different magnetic field strengths. However, simulation of multiquantum powder-pattern lineshapes is associated with problems of nonuniform excitation; moreover, for a certain combination of isotropic chemical-shift value and quadrupole interaction, powder-pattern lineshapes remain overlapped, thus strongly reducing reliability of the multiquantum MAS method.

We shall demonstrate how a combination of double rotation and multiquantum evolution lifts these limitations, provides improved resolution, and opens new analytical possibilities of NMR spectroscopy in the solid state.

The Zeeman energy of a nucleus with spin  $I$  at level  $|m\rangle$  in a rotating coordinate frame can be expressed as

$$E_m = \sigma_0 m + \frac{3}{40} \frac{P_Q^2}{II(2I-1)^2\nu_L} [3n^2 - I(I+1)]m + \Delta[18I(I+1) - 34m^2 - 5]m, \quad [1]$$

where  $\sigma_0$  is the offset from a carrier frequency (in hertz), containing isotropic chemical-shift information, the composite quadrupole-interaction constant is defined as

$$P_Q = \sqrt{(e^2 Qq/h)^2 \left(1 + \frac{\eta^2}{3}\right)}, \quad [2]$$

with conventional quadrupole-interaction parameters (5), and  $\nu_L$  is the Larmor frequency.

The anisotropic term can assume values approximately equal to the isotropic term (6) and depends on the fourth-order spherical-harmonic functions  $R_{40}$  of the particular orientation of the atomic environment as

$$\Delta = \frac{\sqrt{70}}{560} \frac{eQ^2}{II(2I-1)^2\nu_L} R_{40}. \quad [3]$$

A variation of  $R_{40}$ , with explicit form given in many papers ( $I$ , 3) but irrelevant for current purposes, expresses only the anisotropic contribution which is averaged by double rotation but not by MAS.

The pulse sequence for multiquantum signal detection comprised two strong pulses separated by a quadrupole evolution time of 15  $\mu$ s, followed by an evolution period and readout pulse. The effective  $\pi/2$  pulse was about 1.5  $\mu$ s. Phases were chosen such as to observe all transitions in a positive absorption mode (7).

Two-dimensional MAS spectra of  $^{55}\text{Mn}$  in potassium permanganate (Fig. 1) give three lines with characteristic quadrupole lineshape. Positions of the lines on the real axis (in hertz), as derived from Eq. [1] for the case  $I = \frac{5}{2}$ , are given by

$$F_2 = \sigma_0 - \frac{3}{500} \frac{P_Q^2}{\nu_L} + 144\Delta \quad [4]$$

and on the parametric axis by

$$F_1 = 3\sigma_0 - \frac{9}{2000} \frac{P_Q^2}{\nu_L} + 228\Delta$$

$$F_1 = 5\sigma_0 + \frac{3}{80} \frac{P_Q^2}{\nu_L} - 300\Delta \quad [5]$$

for triple- and five-quantum transitions, respectively. A projection perpendicular to line broadening would yield spectra identical to ( $I$ ) where the position of the line is a linear

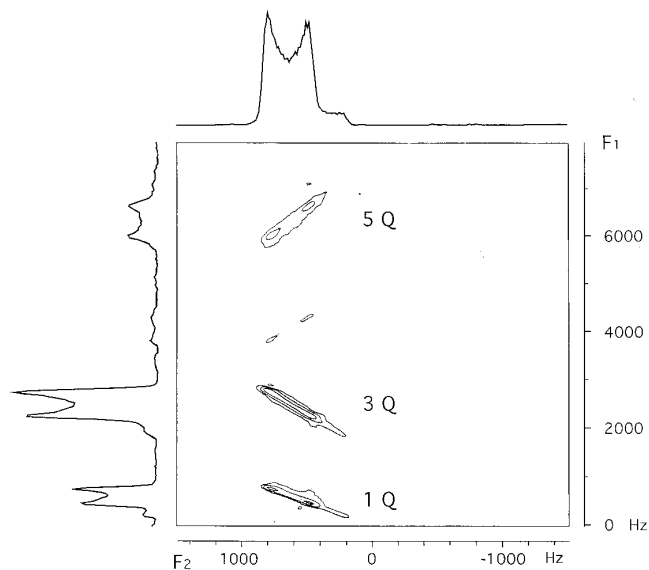


**FIG. 1.** Two-dimensional single-, triple-, and five-quantum MAS NMR spectra of  $^{55}\text{Mn}$  in  $\text{KMnO}_4$  at 49.6 MHz. The parametric  $F_1$  axis is along the vertical.

combination of chemical-shift value via carrier offset with the isotropic second-order quadrupole shift.

Evaluation of quadrupole interaction and chemical shift from Eqs. [4] and [5],

$$\frac{P_Q^2}{\nu_L} = \frac{2000}{27} (F_1 - 3F_2) + \frac{136000}{9} \Delta \quad [6]$$

$$\sigma_0 = \frac{1}{9} (4F_1 - 3F_2) - \frac{160}{3} \Delta \quad [7]$$

for a triple-quantum signal and

$$\frac{P_Q^2}{\nu_L} = \frac{400}{27} (F_1 - 5F_2) + \frac{136000}{9} \Delta \quad [8]$$

$$\sigma_0 = \frac{1}{45} (4F_1 + 25F_2) - \frac{160}{3} \Delta \quad [9]$$

for a five-quantum signal, shows that both multi-quantum transitions carry equivalent information and atomic parameters remain interdependent within the range of possible  $\Delta$  values. Multi-quantum MAS lines overlap if pairs of parameters ( $P_Q$ ,  $\sigma_0$ ) obey

$$3 \frac{P_Q^2}{\nu_L} + 850\sigma_0 = \text{const.} \quad [10]$$

The situation is qualitatively different after application of double rotation, giving average  $\Delta = 0$ . A DOR spectrum

(Fig. 2) exhibits narrow lines of single- and triple-quantum transitions with outer rotation sidebands. The RF field amplitude (an effective  $\pi/2$  pulse of about 4 microseconds) was too weak to excite a five-quantum line because of a much larger coil volume.

From the expressions [6] and [7], the line coordinates immediately enable simultaneous evaluation of chemical shift, i.e., a correction to the original  $F_2$  value, and isotropic second-order quadrupole shift, giving  $P_Q = 1.6$  MHz in agreement with earlier studies (8).

Although multi-quantum lines inherit the line broadening linear with a magnetic field, the two-dimensional stretching of spectra generally improves the resolution due to a different transition dependency of the second-order quadrupole shift. Furthermore, the entire spectral plane can be transformed by double shearing as given by expressions [5]–[8]. Field-independent 2D spectra are obtained if the  $P_Q^2/\nu_L$  axis is multiplied by the Larmor frequency. This is demonstrated on a 3Q DOR spectrum of  $^{27}\text{Al}$  of a mineral nepheline, where the more-abundant of the two sites is characterized by substitutional disorder (9). Two lines overlap slightly in a conventional DOR spectrum, but separate clearly in a canonical representation (Fig. 3). The horizontal axis indicates chemical shift from aqueous solution, and the vertical axis has been transformed in a nonlinear manner to enable a direct readout of the composite quadrupole-interaction constant in the first power. Slices at the left show the quadrupole-interaction lineshape of both sites at the most intense point. Lines in the 2D spectrum along the horizontal axis display the correct chemical shift and are displaced by a different amount from positions in the 1D DOR spectrum, as a result of the respective quadrupole-interaction value.

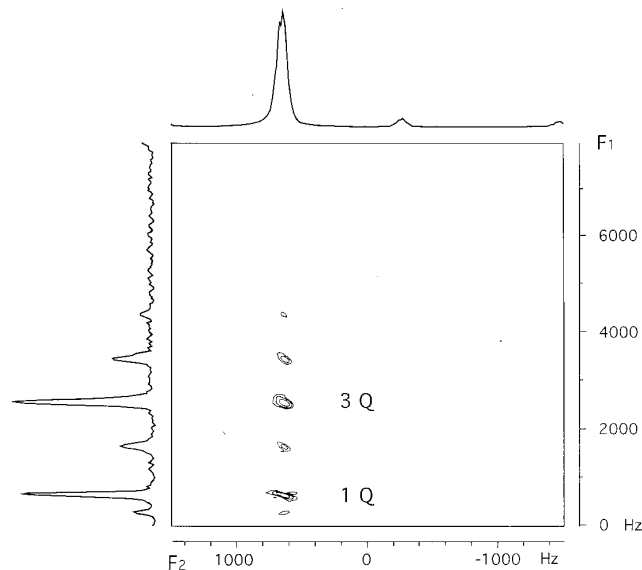


**FIG. 2.** Two-dimensional single- and triple-quantum DOR NMR spectra of  $^{55}\text{Mn}$  in  $\text{KMnO}_4$  at 49.6 MHz. Outer rotor sidebands are visible at 1000 Hz from the triple-quantum centerband.

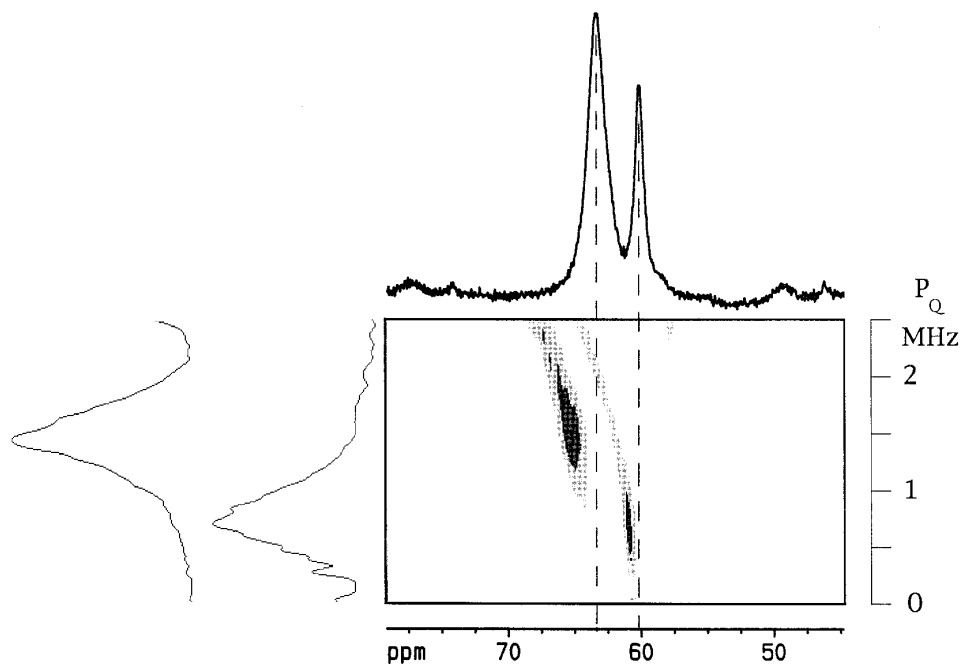


**FIG. 3.** DOR and canonical high-resolution 2D spectrum of  $^{27}\text{Al}$  in nepheline at 93.8 MHz. Peaks along  $F_2$  in the DOR spectrum are located at 63.4 and 60.2 ppm (upper trace), in the canonical spectrum at 64.8 and 60.5 ppm respectively.  $F_1$  slices at 60.4 and 64.8 ppm are shown on the left.

The high-resolution 2D spectra of quadrupole nuclei provide not only for field-independent interpretation of data, but also resolve line-broadening mechanisms and consequently enable an entirely new fingerprinting of materials: correlated spectroscopy of variations in isotropic chemical shift and in the composite parameter of the quadrupole interaction.

#### ACKNOWLEDGMENTS

This work has been supported by my family and Estonian Science Foundation. MAS and DOR probes were prepared by Mr. A. Reinhold and Mr. T. Anupõld, who also assisted in conducting measurements.

#### REFERENCES

1. L. Frydman and J. S. Harwood, *J. Am. Chem. Soc.* 117, 5367 (1995).
2. A. Samoson, E. Lippmaa, and A. Pines, *Mol. Phys.* 65, 1013 (1988).
3. C. Fernandez and J. P. Amoureux, *Solid State NMR* 5, 315 (1996).
4. D. Massiot, B. Touzo, D. Trumeau, J. P. Coutures, J. Virlet, P. Florian, and P. J. Grandinetti, *Solid State NMR* 6, 73 (1996).
5. H. Spiess "NMR Basic Principles and Progress," p. 55, Springer-Verlag, Berlin/New York, 1978.
6. A. Samoson, E. Kundla, and E. Lippmaa, *J. Magn. Reson.* 49, 350 (1982).
7. A. Samoson, *Chem. Phys. Lett.* 247, 203 (1995).
8. M. Wadsworth and P. France, *J. Magn. Reson.* 51, 424 (1983).
9. T. Hahn and M. J. Buerger, *Z. Kristallogr.* 106, 308 (1955).